Competition between quantum fluctuations and antiferroelectric order in Ru-doped $Sr_{0.8}Ca_{0.2}Ti_{1-x}Ru_xO_3$

2009 J. Phys.: Condens. Matter 21 375901

(http://iopscience.iop.org/0953-8984/21/37/375901)

J. Phys.: Condens. Matter **21** (2009) 375901 (7pp) doi:10.1088/0953-8984/21/37/375901

Competition between quantum fluctuations and antiferroelectric order in Ru-doped $Sr_{0.8}Ca_{0.2}Ti_{1-x}Ru_xO_3$

T Wei[1], Y Y Guo[1], Y J Guo[1], S J Luo[1], K F Wang[1], J-M Liu[1,2,3,5], P W Wang[4] and D P Yu[4]

[1] Nanjing National Laboratory of Microstructure, Nanjing University, Nanjing 210093, People's Republic of China
[2] School of Physics, South China Normal University, Guangzhou 510006, People's Republic of China
[3] International Center for Materials Physics, Chinese Academy of Sciences, Shenyang 110016, People's Republic of China
[4] Electron Microscopy Laboratory, Peking University, Beijing 100871, People's Republic of China

E-mail: liujm@nju.edu.cn

Received 31 March 2009, in final form 30 July 2009
Published 13 August 2009
Online at stacks.iop.org/JPhysCM/21/375901

Abstract

The competition between quantum fluctuations and the antiferroelectric state in $Sr_{0.8}Ca_{0.2}Ti_{1-x}Ru_xO_3$ is investigated by measuring the low-temperature dielectric permittivity and by Raman spectroscopy. We demonstrate the significant impact of quantum fluctuations on the stability of the antiferroelectric polar order. It is revealed that the structural phase transitions can be modified by the quantum fluctuations, enhancing the stability of the high-symmetry phase and suppressing the antiferroelectric transitions. More importantly, a quantum antiferroelectric state, exhibiting similar behavior as the quantum ferroelectric state in terms of dielectric response, is identified. In addition, the effect of quantum fluctuations on the increasing permittivity at low temperature is also discussed.

(Some figures in this article are in colour only in the electronic version)

1. Introduction

Strontium titanate $SrTiO_3$ (STO) is a well-known quantum paraelectric [1–3]. It exhibits quantum paraelectricity when the lattice soft mode of incipient ferroelectricity is suppressed by quantum mechanical effects at temperature $T \rightarrow 0$ K. This is a special case of quantum saturation of an order parameter where, upon cooling, the ferroelectric order parameter fails to become non-zero due to quantum fluctuations (QFs) [2, 3]. Mixed $Sr_{1-y}Ca_yTiO_3$ (SCTy) is attractive to researchers because of its rich physics relative to the end members. Structurally, SCTy displays a series of coupled phase transitions, with respect to the single tilting transition of STO at $T \sim 105$ K [4–6]. The phase diagram was constructed recently by means of high resolution neutron and synchrotron x-ray powder diffraction [6].

Mechanically, SCTy displays substantial anomalies in its elastic properties associated with the coupled phase transitions [7–9]. For example, giant elastic anomalies in terms of the shear modulus at ambient conditions, related to a series of symmetry changes $Pm3m \leftrightarrow I4/mcm \leftrightarrow Pbcm \leftrightarrow Pnma$ with increasing $CaTiO_3$ (CTO) content, were observed. Electrically, SCTy can be a quantum paraelectric (QPE), quantum ferroelectric (QFE), relaxor/dipole glass and antiferroelectric (AFE) in the y–T phase diagram [1, 10–13]. While the first three states were extensively investigated, the AFE transition intimately linked with nonpolar antiferrodistortive (AFD) order and driven by the R and M point instabilities in the paraelectric phase was not addressed until recent work for SCTy at $0.18 \leqslant y \leqslant 0.40$ [13].

[5] Author to whom any correspondence should be addressed.

This work confirmed a paraelectric–AFE transition upon cooling down to 100 K. The major issue worth addressing is the instability of the AFE state in SCTy systems against external or internal perturbations.

For example, as a kind of internal perturbation, the quantum fluctuations (QFs) can drive structural transitions in STO, as predicted theoretically. Also, it was predicted that the AFD state is more stable against the QFs than is the ferroelectric (FE) state [14]. This prediction gives rise to a question on the instability of the AFE phase against strong QFs at low T. More interesting is that SCTy at relatively low y exhibits a dielectric anomaly at extremely low T, characterized by the increase in the dielectric permittivity (ε') with decreasing T, and it is noticed that this increase has nothing to do with the QFs themselves. Therefore, one is concerned with the origin of this increasing phenomenon and its response to the QFs. These issues remain essentially unclear and knowledge of the effect of the QFs is helpful for understanding them [13].

So far, the structural phase transitions of SCTy in the AFE region were addressed [4–6], but not much work dealing with the effect of QFs on the AFE state and the related dielectric anomaly has been reported. Such a motivation is of significance not only from the point of view of the fundamental physics but also from the perspective of technical applications [1–3, 15, 16]. In this work, we pay attention to the influence of QFs stimulated by Ru doping in $Sr_{0.8}Ca_{0.2}Ti_{1-x}Ru_xO_3$ (SCTR). The competition between the QFs and the AFE polar order will be confirmed. It will be demonstrated that the AFE phase transitions can be tuned by the QFs, thereby enhancing the stability of the high-symmetry phase and suppressing the AFE transitions. The AFE state will eventually transit into the QPE state, passing by a quantum antiferroelectric (QAFE) state. Furthermore, it is also proven that the low-temperature increasing region below the AFE order is sensitive to the QFs.

2. Experimental details

Before going into details of our experiments, we would like to note that there remain some challenges in dealing with the QFs (e.g. in STO) due to the complexity [17]. Theoretically, a full-scale approach to the QFs seems unavailable while the transverse Ising model has been extensively employed. One may also treat the QFs using a simple semi-quantum-mechanical resonator, although it may not be quantitatively accurate. Interestingly, this simple model does predict the effect of Ru doping in SCTR, as we shall see here. Furthermore, this explanation can in principle be applied to doping of other transition elements with d electrons, i.e. Mn^{3+} and Fe^{3+}. Experimentally, to investigate the effect of the QFs, it is necessary to resolve how to characterize the QPE state which is usually characterized by three types of behavior. First, the long-wavelength, transverse optic phonon mode cannot be frozen even as $T \rightarrow 0$ K, due to the QFs [18, 19]. Second, dielectric permittivity ε' increases with decreasing T until a threshold (∼4 K for STO), below which ε' levels off and forms an ε'–T plateau, due to the QFs [1–3, 20]. Third, if the QFs are sufficiently strong, the AFE state may be suppressed and a AFE–QPE transition will occur, by which the (anti)ferroelectric phonon modes will disappear. The long-wavelength phonon mode has very low wavenumber (∼50 cm^{-1} or lower) and cannot be reached by conventional Raman spectroscopy. Terahertz or infrared spectroscopy may be appropriate techniques for detecting this mode, although the signal is usually very weak. Unfortunately, such highly reliable spectroscopy run at low T is not available to us and we alternatively characterize the dielectric plateau and stability of the AFE phonon modes in order to identify the quantum paraelectricity, as usually done by other researchers.

In our experiments, polycrystalline SCTRs with $x = 0$, 0.01, 0.02, 0.03, 0.045, 0.05 and 0.06 were synthesized by the solid-state reaction method [21]. X-ray diffraction (XRD) with Cu Kα radiation indicated all the samples have a perovskite structure at room temperature and no secondary phase was found. The dielectric property was measured using an HP4294A impedance analyzer by inserting the samples into the Janis closed-cycle refrigerator system (Janis Research Company, Inc., USA). To check the ferroelectric stability of the samples at various T, Raman spectroscopy was undertaken using a Renishaw inVia Raman microscope with an Ar ion laser (514 nm) source.

3. Results and discussion

3.1. Dielectric behaviors

Figure 1 displays the measured $\varepsilon'(T)$ for all the samples at different frequencies from 1 kHz to 1 MHz. Clearly, no frequency dispersion for $\varepsilon'(T)$ was observed over the whole frequency and temperature ranges for the measurements, noting that the T axis is in log-scale. We focus on two features, as shown in figure 1(a) for the sample $x = 0$ (i.e. pure SCT). First, the broad peak at $T_C = 106$ K originates from the AFE transition driven by the phonon instability at the Δ point of the cubic Brillouin zone, due to the small antiparallel displacements of Ti^{4+} and Sr^{2+}/Ca^{2+} ions along the [010] direction on the (001) plane of the ideal cubic perovskite [13]. Second, a continuous increase of $\varepsilon'(T)$ with decreasing T, starting at $T \sim 80$ K, was observed. Although the nature of this feature is unclear, it would not be the consequence of the QFs, since we will show later that the Ru doping does not enhance and extend this increasing trend but suppresses it into a QF-dominated broad plateau.

We look at the effect of Ru doping on $\varepsilon'(T)$, as plotted in figures 1(b)–(g), respectively. The evolution of $\varepsilon'(T)$ is characterized by two distinct effects. With increasing x from 0.0 to 0.06, the AFE peak shifts towards the low-T side and its height is suppressed. On the other hand, the increased permittivity at the low T is continuously suppressed in height and evolves into a plateau with its width extending toward the high-T side. Eventually, the two features merge into a broad plateau covering $T = 0$–40 K at $x = 0.06$, a typical effect for a QPE.

The suppression of the AFE peak reflects destabilization of the AFE state, while a similar comment applies to the

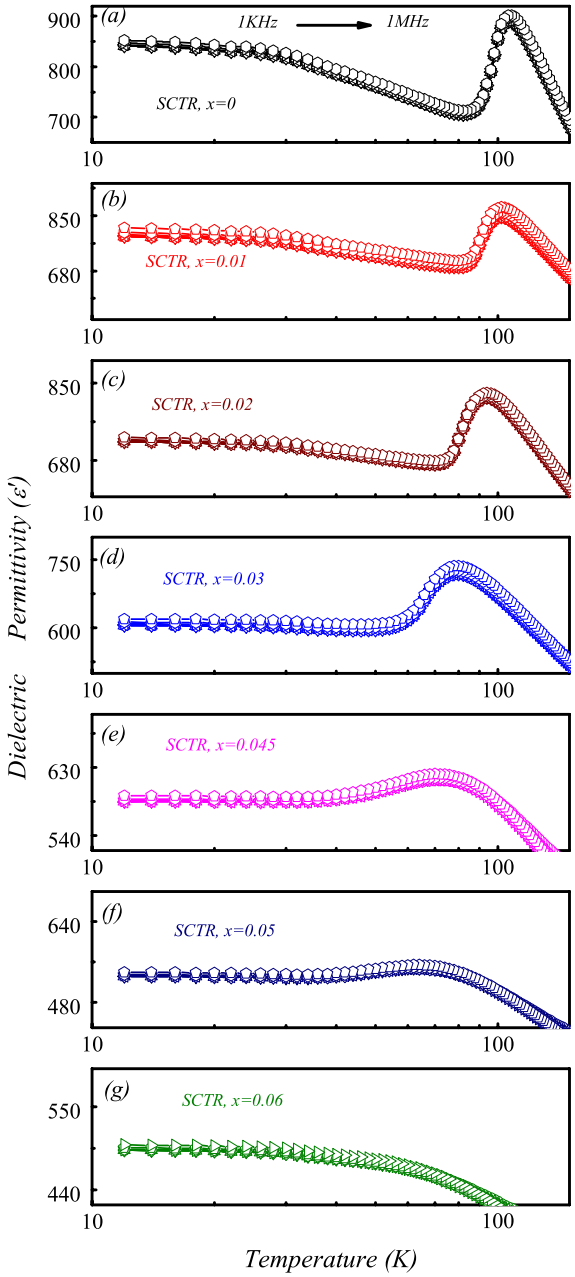

Figure 1. Measured ε' at different frequency (1 kHz to 1 MHz) as a function of T for all the samples ((*a*)–(*g*)).

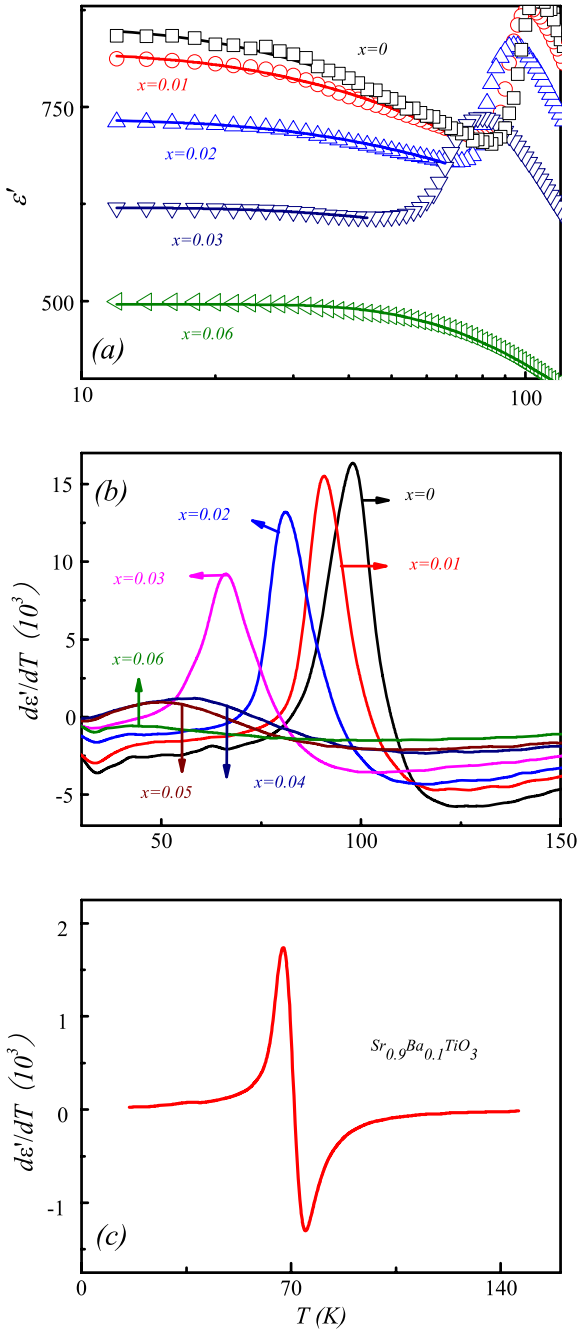

Figure 2. ε'–T plots and the fitting results (solid curves) using equation (1) for the low-T range (*a*). Variation of $\mathrm{d}\varepsilon'/\mathrm{d}T$ versus T for all SCTR samples and $Sr_{0.9}Ba_{0.1}TiO_3$ ((*b*) and (*c*), respectively).

increase in permittivity at the low-T range. Since the doping enhances the QFs, to be addressed below, the remarkable effect of the QFs on the AFE order is demonstrated. In addition, one may argue that the doping seriously deteriorates the polarization of SCTR, referring to the decreasing ε'. To characterize this effect, the Barrett equation is used to fit $\varepsilon'(T)$ data in the permittivity increasing range at low-T [20]:

$$\varepsilon' = C/\{(T_1/2)\coth(T_1/2T) - T_0\}, \qquad (1)$$

where C is the Curie constant, T_1 represents the tunneling integral and T_0 is the transition temperature for the dipole order (FE or AFE order). The best fittings of the data are given by the solid lines in figure 2(*a*) and the evaluated C, T_1 and T_0 are listed in table 1. Note that no fitting to samples of $x = 0.045$ and 0.05 was done, since the tail of the AFE peak is going to merge with the dielectric plateau in the low-T side, with the result that any fit using the Barrett equation would not be reliable.

For $x = 0$, the fitted $(T_1 - 2T_0)$ is positive, indicating that the increase in permittivity at the low-T range is already dominated by the QPE state, i.e. the QFs are remarkable at very low T. For $0 < x \leqslant 0.03$, the monotonic increasing of T_1 and decreasing T_0 with increasing x indicates significantly enhanced QFs. The very positive $(T_1 - 2T_0)$ implies enhanced

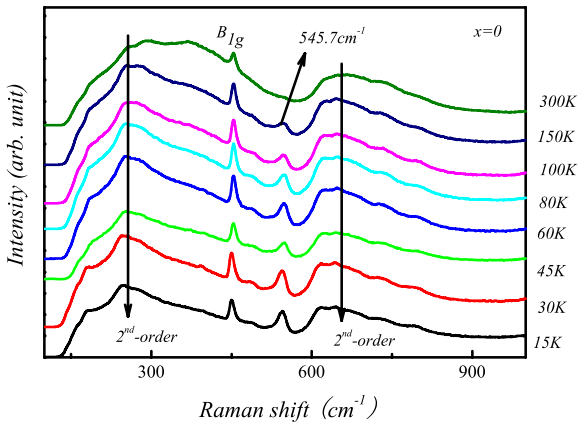

Figure 3. Raman spectra for $x = 0$ at various temperatures.

Table 1. Parameters C, T_1 and T_0 evaluated from fitting of $\varepsilon'(T)$ using the Barrett equation. The numbers in the parentheses are uncertainties of fitting.

Samples	C (10^5)	T_1 (K)	T_0 (K)	$T_1 - 2T_0$ (K)
SCTR00	2.5(0.1)	37(4)	−273(13)	583
SCTR01	2.8(0.1)	40(4)	−327(19)	694
SCTR02	3.8(0.2)	50(3)	−512(26)	1074
SCTR03	4.9(0.6)	73(4)	−754(96)	1581
SCTR06	1.0(0)	180(1)	−102(3)	385

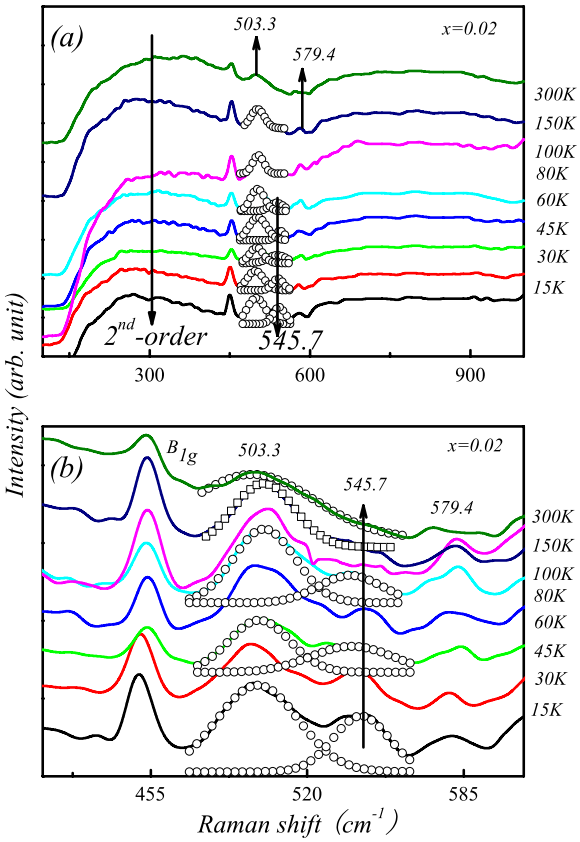

Figure 4. Raman spectra for $x = 0.02$ at various temperatures (a). The magnified part of the Raman spectra in (a) is given in (b) for clarification.

stability of the QPE state with increasing x [20, 22]. This tendency is expected to continue for $x = 0.045$ and 0.05, although the AFE state remains competitive with the QPE state. When x increases up to 0.06 and above, the QFs completely suppress the AFE state and only the QPE state is identified in the low-T range [20, 22]. Therefore, the QFs induced by Ru doping can suppress the AFE state, and the increase in permittivity at low T can also be merged away.

Furthermore, figure 2(b) gives $\mathrm{d}\varepsilon'/\mathrm{d}T$ as a function of T for all SCTR samples. For $x = 0$, there is an obviously abnormal peak located at $T \sim 98$ K, which should correspond to the low-T side of the AFE phase transition in figure 1(a). In contrast, the diffusive shallow minimum centered on $T \sim 124$ K is believed to be due to the high-T side of the AFE phase transition. Here, one notes that this behavior is different from the case of ferroelectric $Sr_{0.9}Ba_{0.1}TiO_3$, as shown in figure 2(c). The intense peak of $\mathrm{d}\varepsilon'/\mathrm{d}T$ at $T \sim 98$ K corresponds to the sharply reduced dielectric permittivity due to the freezing of AFE polar order. With increasing x, the $\mathrm{d}\varepsilon'/\mathrm{d}T$ peak shifts towards the low-T side and its height also decreases, and the peaks become broader and more dispersive, corresponding to gradual melting of the long-range AFE state. These results are self-consistent with the dielectric data. Therefore, with increasing x, the stimulated QFs begin to play a dominant role and suppress the AFE structural phase transition, favoring the high-symmetry QPE phase.

3.2. Raman spectroscopy

More evidence supporting the preference of the QPE state over the AFE state is provided by the disappearance of the Raman phonon modes associated with the AFE order. Figures 3–5 present the Raman spectra for $x = 0$, 0.02 and 0.06 at several T, respectively. In figure 3 at $x = 0$ (pure SCT), the two broad bands centered at ∼300 and 650 cm^{-1} are due to the second-order Raman scattering [13]. The peak at ∼450 cm^{-1} is the first-order Raman B_{1g} mode, indicating the non-cubic perovskite structure of SCT at $T = 300$ K. Below $T = 150$ K, a new Raman peak centered at ∼545 cm^{-1} appears, relating to the AFE phase [23]. Figure 6 plots the intensity of this phonon mode as a function of T, normalized both by the Bose factor $n + 1 = [1 - \exp(-h\omega)/2\pi kT]^{-1}$, where h is the Planck constant, ω is the phonon frequency, k is the Boltzmann constant, and by the intensity of the corresponding mode at $T = 15$ K [21]. A rapid enhancement of the intensity near 110 K, the AFE transition point from the high-T paraelectric phase, is clearly shown.

Figure 4(a) gives the spectra for doped sample $x = 0.02$. The hard B_{1g} mode remains active, indicating the non-cubic perovskite structure over the whole T range, while the two second-order bands are slightly suppressed by the doping. Furthermore, the 545 cm^{-1} AFE mode does not appear until $T \sim 80$ K, also consistent with the dielectric data, indicating the AFE transition at this temperature. What should be noted here is the two new modes centered at ∼503.3 and 579.4 cm^{-1}. The 503.3 cm^{-1} mode overlaps partially with the 545 cm^{-1} AFE mode to form an overlapped peak, as shown in figure 4(b) for clarification, and one needs to separate the two modes.

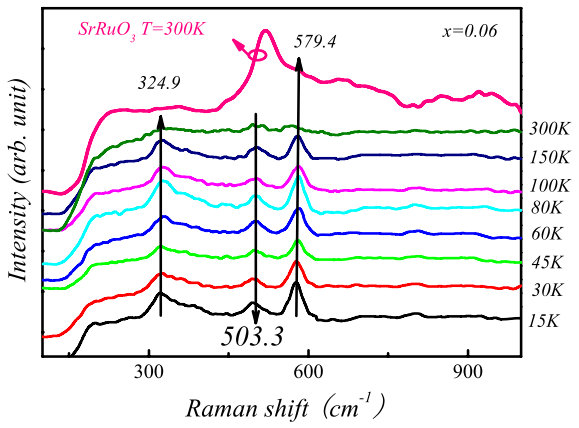

Figure 5. Room temperature Raman spectrum for $SrRuO_3$ and Raman spectra for $x = 0.06$ at various temperatures.

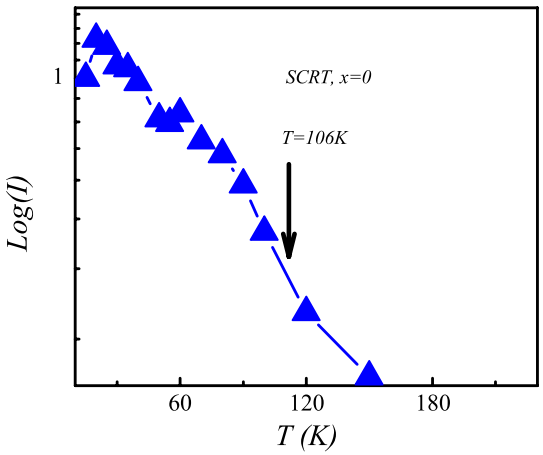

Figure 6. Measured normalized Raman intensity (I) of the AFE mode at 545 cm^{-1} as a function of T for pure SCT sample, and the solid curves are guides for the eyes.

To proceed, it is noted that the Raman lines usually become broader upon doping, because the doping will induce lattice defects. The scattering from the defects contributes to the lineshape in different forms, and eventually the lineshape takes a Lorentzian profile [24]. Therefore, the Lorentzian fitting is used to separate the two overlapped modes. We present in figure 4(*b*) the Raman spectra of sample $x = 0.02$ where the 545 cm^{-1} AFE mode is separated from the overlapped peak by the fitting. Indeed, the two broad second-order Raman bands and the hard B_{1g} mode (existing in pure SCT) have disappeared, and the 545 cm^{-1} AFE mode is also absent, indicating the AFE phonon mode is suppressed, a fact consistent with the dielectric plateau in figure 1.

Besides the disappearance of the 545 cm^{-1} AFE mode, we identify three other Raman modes: 324.9, 503.3 and 579.4 cm^{-1}. These modes are visible at room temperature and become well identified below $T = 150$ K. To understand the origin of these modes, the Raman pattern for polycrystalline $SrRuO_3$ was measured and the data at 300 K are shown in figure 5 for comparison (coarse red curve). It is seen that $SrRuO_3$ exhibits very broad peaks around ~300 cm^{-1} and in between 500 and 700 cm^{-1}. Clearly, the three Raman modes (324.9, 503.3 and 579.4 cm^{-1}) are non-AFE-related and can be assigned to the contribution from $SrRuO_3$ units in the $x = 0.06$ sample.

3.3. Origin of enhanced quantum fluctuations

We come to explain the enhanced QFs and AFE destabilization induced by Ru doping. Usually, for such a doping, two possible mechanisms can be suggested. First, the partially filled d electrons of Ru may interact with the AFE phonon modes and harden these modes, which thus enhances the QFs and suppresses the AFE state [25]. Second, doping of ions with partially filled d orbitals restricts the shift of the ions from the center of O_6 octahedra [26]. Here, we propose a simple model in the framework of semi-quantum-mechanical resonators, to account for the enhanced QFs. Consider a dynamical Hamiltonian of the general form

$$\mathrm{H} = \sum_{i}^{n} p_i^2/2m_i + V(\mu_1, \mu_2, \ldots, \mu_i, \ldots, \mu_n), \qquad (2)$$

where p_i, μ_i and m_i represent the ith particle momentum, coordinate and mass, and V is the total potential energy [1]. For $SrTiO_3$, the presence of the momentum coordinates p_i in equation (2) which do not commute with μ_i, i.e.

$$\{p_i, \mu_j\} = \mathrm{i}\hbar\delta_{ij}, \qquad (3)$$

suppresses the phase transition due to the nonvanishing zero-point motion [1], i.e.

$$E_0 = \frac{1}{2}\frac{h}{2\pi}\omega = \pi\hbar\nu = \pi\hbar\sqrt{\frac{k}{m}}, \qquad (4)$$

where h is the Planck constant, ω is the vibration frequency, and k and m are respectively the elasticity coefficient and reduced mass of an equivalent classical harmonic oscillator (B–O bond in the ABO_3 structure). In addition, within the framework of a classical resonator, the energy of a harmonic oscillator can also be described by equation (5):

$$E_0 = \tfrac{1}{2}kA^2, \qquad (5)$$

where A is the vibration amplitude. Thus, combining equations (4) and (5) yields

$$A^2\sqrt{km} = C, \qquad (6)$$

where C is a constant.

From equation (6), we know that the value of A can qualitatively characterize the degree of QFs [27]. Thus, for the present SCTR system, we need to evaluate the values of k and m in order to obtain the strength of QFs. Here, k and m can be simply obtained by considering a balance between the electric charge bond energy and E_0, resulting in $k = 2U_{\mathrm{bond}}/r^2$, where U_{bond} is the B–O bond energy supposed to be contributed mainly by the Coulomb energy and r is its separation. For

the Ru–O and Ti–O bonds in SCTR, $U_{\text{bond}} = 672.4$ kJ mol^{-1} for the Ti–O bond and 528.4 kJ mol^{-1} for the Ru–O bond, and $r = 0.1953$ nm [28], we immediately have $k_{\text{Ru–O}}/k_{\text{Ti–O}} = 0.7858$. By taking the effective masses of the two types of bonds, we have $A^2(\text{Ru–O})/A^2(\text{Ti–O}) = 1.0511$, indicating a 2.6% increase of the Ru–O vibration amplitude with respect to the Ti–O bond in SCTR.

As we know, the FE or AFE phase transition in the perovskite structure is a collective behavior of dipoles. Thus, the lattice vibration of the Ti atoms will be determined by their collective bonding within the Ti–O octahedra. The Ru doping will influence the lattice vibration mode of the Ti–O bond, which is an average effect. Note that, though we did not observe the soft mode for the SCTRx system owing to the instrumental limitation, the reduction of dielectric constant may suggest the hardening of the soft mode in frequency due to the Ru doping, according to the Lyddane–Sachs–Teller (LST) relationship. This is also consistent with the enhanced QFs in this system. In a qualitative sense, we believe that a ~2.6% increase of the vibration amplitude of the Ru–O bond can enhance the collective average frequency for this particular lattice mode, i.e. suppressing the FE/AFE stability, referring to the static displacement for the FE state in $BaTiO_3$ is only ~0.5% of the bond length. Therefore, the Ru doping can stimulate the QFs and break the AFE state in SCTR. In fact, for doping of other ions of partially filled d electrons, e.g. Fe^{3+} and Mn^{3+} [29], a similar argument can be made, although it may not be accurate since the present model seems to be oversimplified for such strongly correlated electron oxides.

3.4. Phase diagram

In order to clearly display the interaction between AFE and QFs, figure 7 displays the T–x phase diagram for the current SCTR system. The AFE phase transition temperature is about ~108 K for pure SCT. Above this temperature, it is orthorhombic with space group $Pbnm$ [2, 4–6]. The closed red triangles correspond to the AFE transition temperature (T_C) as a function of x. The decreasing T_C with increasing x indicates the impact of the QFs on the AFE polar instability. Furthermore, the closed green circles represent the temperature corresponding to the dielectric peak in figure 2(*b*). This temperature is also the melting point of the AFE order, defined by T_P, as shown in figure 7. It is shown that the AFE phase is gradually melted by the enhanced QFs. Below ~80 K for pure SCT, an abnormal increase in permittivity at low T appears, being attributed to the influence of the abnormal phase (AP). The corresponding temperature is labeled as T_{AP} here. The variation of T_{AP} with x is clearly shown in figure 7 by the closed brown pentagons. Due to the stimulated QFs induced by the Ru doping, the abnormal phase is seriously suppressed. It is clearly shown by the decrease of the AP region with increasing x. More importantly, the influence of the QFs (represented by T_1) as a function of x is also shown in figure 7 with the blue closed square symbols. The stimulated QFs increase rapidly with x and play a significant role in competition with the AFE state or AP.

Finally, we deal with the dynamics of the AFE–QPE transitions. It is established that the FE state coexisting with strong QFs can be defined as a QFE state [1, 27, 30]. The issue of how the AFE state in pure SCT transits into the QPE state is important. Figure 7 gives the AFE transition point T_C as a function of x. This dependence can be fitted by a scaling: $T_C = 397.6 \times (0.07 - x)^{1/2}$, as displayed by the open circle line in figure 7. This scaling was predicted and experimentally confirmed for the QFE state, taking account of the strong QFs involved [1, 27, 30]. A similar prediction can be made in the present case where strong QFs are involved in the AFE–QPE transition, which suggests that the transition is probably accompanied by a quantum antiferroelectric (QAFE) state for $x > 0$. It should be noted that the fitted scaling relation predicts a critical value of $x \sim 0.07$ at which the QPE state is arrived at, roughly consistent with $x = 0.06$ at which the AFE state is completely suppressed.

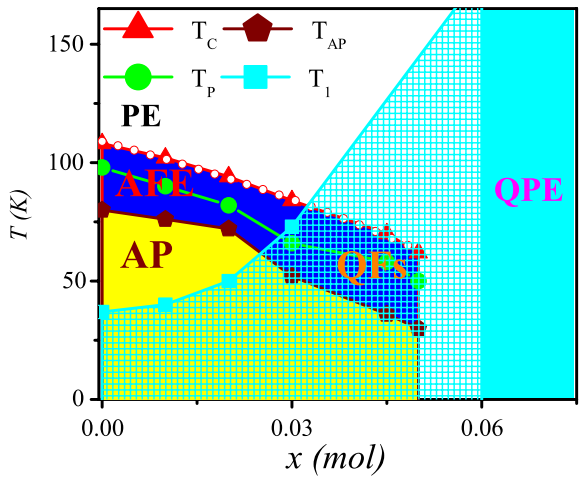

Figure 7. T–x phase diagram for current SCTR system. The symbols are experimental data and the solid curves are guides for the eyes. The open circle line is the fitting results for the QAFE state.

4. Conclusion

In conclusion, the competition between the QFs and AFE state in SCTR has been revealed through the dielectric and Raman spectroscopies over a broad T range. It has been demonstrated that the low-symmetry AFE phase is modified by the QFs which enhance the stability of the high-symmetry phase and reduce the transition temperature. Furthermore, the QAFE state, which shows similar behavior to the QFE state, is identified. In addition, it has been revealed that the low-T increase of the dielectric permittivity is sensitive to the QFs.

Acknowledgments

This work was supported by the National Natural Science Foundation of China (50832002, 50601013 and 50528203) and the National Key Projects for Basic Researches of China (2009CB623303 and 2006CB921802).

References

[1] Müller K A and Burkard H 1979 *Phys. Rev.* B **19** 3593
[2] Salje E K H, Wruck B and Thomas H 1991 *Z. Phys.* B **82** 399

[3] Rytz D, Höchli U T and Bilz H 1980 *Phys. Rev.* B **22** 359
[4] Yamanaka T, Hirai N and Komatsu Y 2002 *Am. Mineral.* **87** 1183
[5] Gallardo M C, Becerro A I, Romero F J, Cerro J D, Seifert F and Redfern S A T 2003 *J. Phys.: Condens. Matter* **15** 91
[6] Carpenter M A, Howard C J, Knight K S and Zhang Z 2006 *J. Phys.: Condens. Matter* **18** 10725
[7] Kityk A V, Schranz W, Sondergeld P, Havlik D, Salje E K H and Scott J F 2000 *Phys. Rev.* B **61** 946
Kityk A V, Schranz W, Sondergeld P, Havlik D, Salje E K H and Scott J F 2000 *Europhys. Lett.* **50** 41
[8] Harrison R J, Redfern S A T and Street J 2003 *Am. Mineral.* **88** 574
[9] Carpenter M A, Li B and Liebermann R C 2007 *Am. Mineral.* **92** 344
[10] Zhang L, Zhong W-L and Kleemann W 2001 *Europhys. Lett.* **53** 401
[11] Kleemann W, Dec J and Westwanski B 1998 *Phys. Rev.* B **58** 8985
[12] Levstik A, Filipic C, Bobnar V and Pirc R 2003 *Ferroelectrics* **295** 633
[13] Ranjan R, Pandey D and Lalla N P 2000 *Phys. Rev. Lett.* **84** 3726
[14] Zhong W and Vanderbilt D 1996 *Phys. Rev.* B **53** 5047
[15] Grupp D E and Goldman A M 1997 *Science* **276** 392
[16] Takesada M, Yagi T, Itoh M and Koshihara S 2003 *J. Phys. Soc. Japan* **72** 37
[17] Lemanov V V 2002 *Ferroelectrics* **265** 1
[18] Taniguchi H, Itoh M and Yagi T 2007 *Phys. Rev. Lett.* **99** 017602
[19] Holder A B and Bishop A R 2008 *Phys. Rev.* B **78** 104117
[20] Barrett J H 1952 *Phys. Rev.* **86** 118
[21] Wei T, Guo Y J, Wang P W, Yu D P, Wang K F, Lu C L and Liu J-M 2008 *Appl. Phys. Lett.* **92** 172912
Wei T, Zhu C, Wang K F, Cai H L, Zhu J S and Liu J-M 2008 *J. Appl. Phys.* **103** 124104
[22] Tkach A, Vilarinho P M and Kholkin A L 2005 *Appl. Phys. Lett.* **86** 172902
[23] Ouillon R, Lucarre J P P, Ranson P, Pruzan P, Mishra S K, Ranjan R and Pandey D 2002 *J. Phys.: Condens. Matter* **14** 2079
[24] Kirillov D and Reynolds G J 1994 *Appl. Phys. Lett.* **65** 1641
[25] Zhi Y and Chen A 2001 *Appl. Phys. Lett.* **80** 643
[26] Khomskii D I 2006 *J. Magn. Magn. Mater.* **306** 1
[27] Schneider T, Beck H and Stoll E 1976 *Phys. Rev.* B. **13** 1123
[28] Lide D R 2003 *Handbook of Chemistry and Physics* 84th edn (Boca Raton, FL: CRC press)
[29] Tkach A, Vilarinho P M and Kholkin A 2004 *Ferroelectrics* **304** 87
[30] Fu D, Itoh M, Koshihara S Y, Kosugi T and Tsuneyuki S 2008 *Phys. Rev. Lett.* **100** 227601